PAN ARCHIVES OF ACOUSTICS
Vol. **42**, No. 2, pp. 297–311 (2017)

DOI: 10.1515/aoa-2017-0032

Calibration and Laboratory Testing of Computer Measuring System 8AE-PD Dedicated for Analysis of Acoustic Emission Signals Generated by Partial Discharges Within Oil Power Transformers

Franciszek WITOS[(1)], Grzegorz SZERSZEŃ[(2)], Zbigniew OPILSKI[(1)], Maciej SETKIEWICZ[(1)]
Aneta OLSZEWSKA[(1)], Dominik DUDA[(3)], Krzysztof MAŹNIEWSKI[(3)], Marek SZADKOWSKI[(3)]

[(1)] *Department of Optoelectronics, Faculty of Electrical Engineering*
Silesian University of Technology
Krzywoustego 2, 44-100 Gliwice, Poland; e-mail: Franciszek.Witos@polsl.pl

[(2)] *State Higher Vocational School in Tarnow*
Department of Electronics and Telecommunications
Mickiewicza 8, 33-100 Tarnów, Poland

[(3)] *Institute of Power System and Control, Faculty of Electrical Engineering*
Silesian University of Technology
Krzywoustego 2, 44-100 Gliwice, Poland

(*received August 22, 2016; accepted April 6, 2017*)

In the paper, there are presented a general description of the constructed measuring system 8AE-PD, the results of calibration of this system by the Hsu-Nielsen method as well as the testing of the measuring system during recording signals generated by Hsu-Nielsen sources in a steel plate and a modeled partial discharge (PD) source.

There is also presented the methodology of investigations by the calibrated acoustic emission method. The results of analyses of PD signals coming from the modeled sources are given. In particular, there are described the properties of acoustic emission (AE) signals generated by the PDs as well as the dependencies of the peak-to-peak voltage U_{mm}, the RMS voltage U_{rms} and the descriptors of acronyms ADP and ADC on the apparent charge Q introduced by the modeled PD source. There are determined the limit values of the apparent charge Q introduced by the modeled PD source for which the recorded signal is identified as originating from the PDS.

Keywords: multichannel system; calibration; acoustic emission; partial discharge; power oil transformers.

1. Introduction

Acoustic emission has been the authors' area of interest for over 30 years. The investigations performed by the authors include the analysis of signals generated in selected geological materials (Malecki *et al.*, 1993), in selected deformation processes (partial discharges) (Witos, 2008) as well as applications of the acoustic emission method in coal walls (Opilski *et al.*, 1985), conveyor belts (Witos *et al.*, 1989), hydrogenerator coil bars (Witos, Gacek, 2013) and oil power transformers (Witos, Gacek, 2008; 2009). For the purpose of recording acoustic emission signals, analyzing the recorded signals and developing applications, the authors have introduced a number of modifications of the measuring equipment and have developed the software which provides monitoring and recording the signals as well as their advanced analysis. Based on the acquired experience, the authors have designed and constructed the measuring system 8AE-PD for investigations of partial discharges in oil power transformers. This system is presented in detail in (Witos *et al.*, 2012). In this paper, the system is described in a general way, whereas the issues of its calibration and testing as well as its application to laboratory investigations of partial discharges generated by the modeled sources are presented in detail.

2. The computer measuring system 8AE-PD for investigating partial discharges by the acoustic emission method

Figures 1 and 2 show schematic and block diagrams of the constructed measuring system 8AE-PD for investigating partial discharges in oil power transformers. The system is equipped with eight fully independent measurement channels so that one can simultaneously record signals at eight measurement points selected on the tested object. The system consists of preamplifiers, CPU, software as well as a computer and AE sensors.

The system operates as follows: signals recorded by the AE sensors are pre-amplified in independent preamplifiers and applied to the inputs of amplifiers (inputs CH0–CH7). The central unit contains instrumentation amplifiers, a system of forming the reference voltage, a microcontroller and a PXI 1033 chassis including a PXI 6133 measuring card together with a power supply and an MXI-Express integrated controller (National Instuments Corporation).

The complete software developed for the measuring system enables monitoring and recording signals – program "Monitor PXI-6133 v11", the fundamental analysis of the recorded signals – program "DEMA Analyzer v.8" and the advanced analysis of the recorded signals – program "Amplitude distributions and AE descriptors". It should be emphasized that the data written in the program "Monitor PXI-6133 v11" and read in "DEMA Analyzer v.8" are recalculated in individual measurement channels directly at the preamplifier input. As the result, the further analysis is independent of the gain chosen during measurements in individual measurement channels of the measuring system 8AE-PD. It is therefore the analysis of the signals directly at the AE sensor output. Such an approach allows one to better compare the investigated phenomena.

The preamplifiers were designed and manufactured to cooperate with D9241A AE sensors produced by Physical Acoustic Corporation. The D9241As have differential outputs and a dual BNC connector per output. They have very good EMI shielding ability and provide high common noise rejection and low noise, even in electrically noisy environments. These sensors are typically used for monitoring large power transformers.

The measuring system 8AE-PD was designed in such a way that the cooperation with R6 an WD sensors made by the PAC company, used in the system DEMA-COMP (Witos *et al.*, 2011; Olszewska, Witos, 2012) so far, is possible.

The detailed description of the constructed measuring system is presented in (Witos *et al.*, 2012).

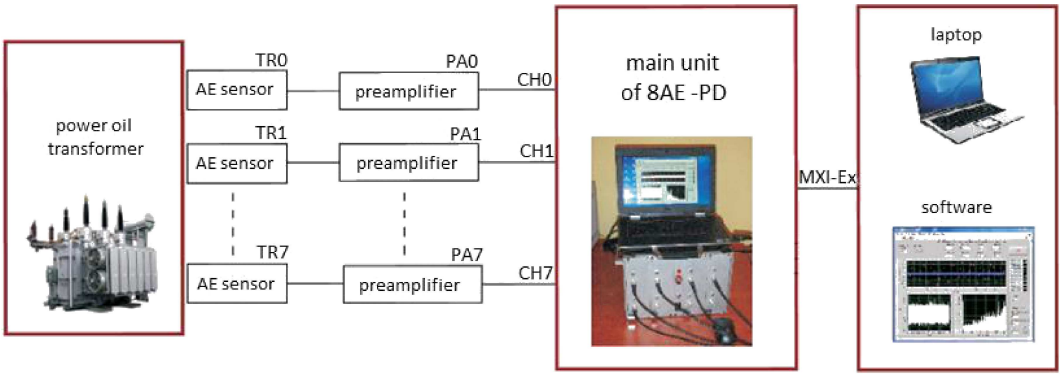

Fig. 1. Basic schematic diagram of the measuring system with the computer system 8AE-PD.

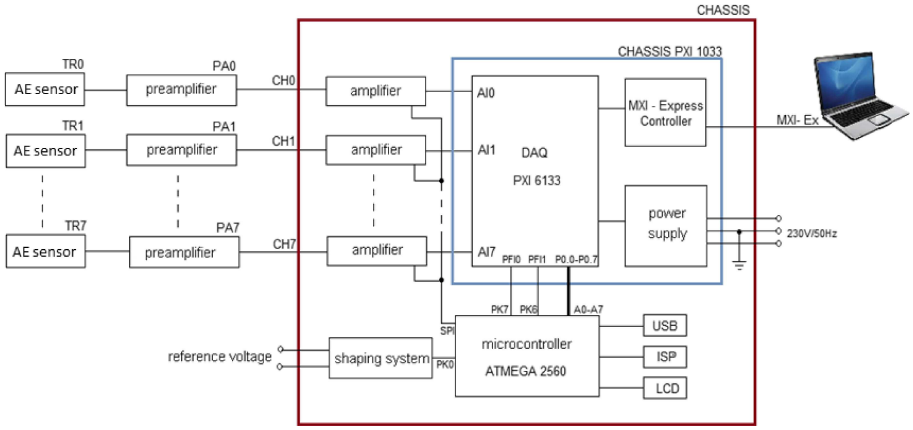

Fig. 2. Block diagram of the measuring system 8AE-PD.

3. Calibration of the measuring system 8AE-PD

During the calibration of the measuring system, there were used two methods for generating the reference pulse signals (Hsu, Breckenridge, 1981; Ranachowski, 1992; Skubis, 1993): the method in which a metal ball is dropping on the test plate is the source of signal and the Hsu-Nielsen method (breaking a 0.5 mm 2H graphite lead placed in an automatic pencil with appropriate teflon coated tip). Example signals recorded during investigations using both methods and their amplitude-frequency characteristics are shown in Figs. 3b and 3c.

The detailed analysis of the properties of the recorded signals shows that the frequency bands occurring in the signals recorded during the Hsu-Nielsen test are consistent with the frequency bands of the PD signals recorded by the AE method in oil power transformers (Boczar, 2001; MacAlpine, 2002; Sarathi *et al.*, 2007; Witos *et al.*, 2011). Due to that result, the system was calibrated by the Hsu-Nielsen method.

The essence of calibration is to calculate corrections of gains $\Delta K_u(x)$ in particular measurement channels, and next introduce these corrections as a parameter of the measuring system to ensure an identical amplitude response in each measurement channel.

The measurement procedure of the measuring system calibration consisted in recording the signals coming from ten Hsu-Nielsen events (breaking a 0.5 mm 2H graphite lead placed in an automatic pencil with appropriate teflon coated tip). During the calibration, the Hsu-Nielsen source was at the point S (Fig. 4), whereas the AE sensors were placed at the distance of 50 cm from the source.

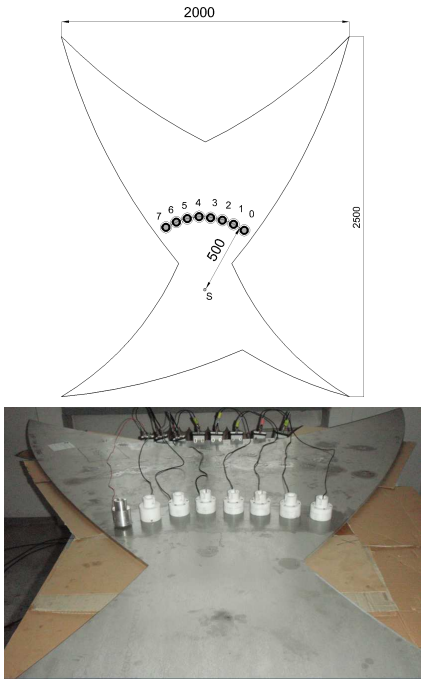

Fig. 4. Arrangement of AE sensors on the surface of the steel plate during calibration by the Hsu-Nielsen method: 0–7 positions of AE sensors, S – position of the Hsu-Nielsen source.

a) noise

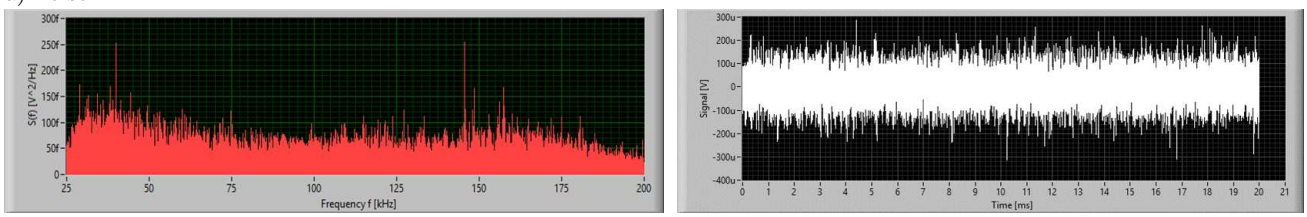

b) falling ball

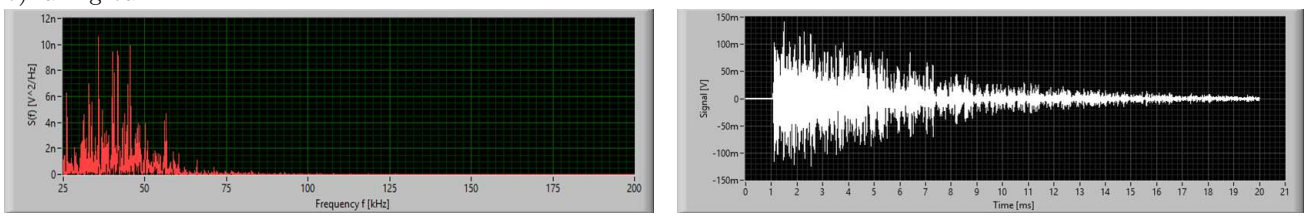

c) Hsu-Nielsen test

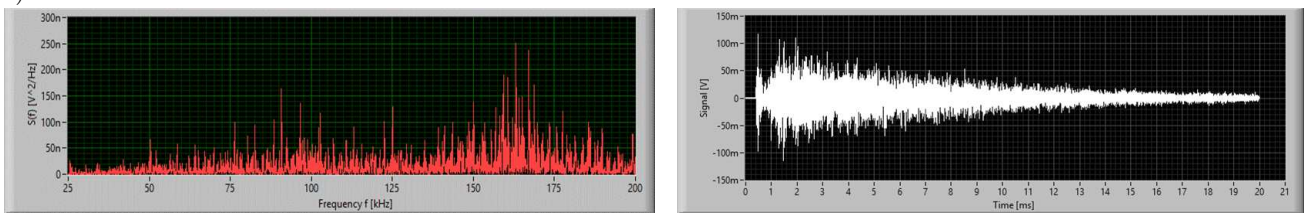

Fig. 3. Signals recorded with a WD wide-band AE sensor in channel CH6 together with the amplitude-frequency characteristics for the following measurement conditions (band 25–200 kHz, the filtr of 5th order, measuring circuit CH6: preamplifier #6, AE sensor of WD): a) noises in the measurement channel, b) the modeled AE source in the form of the dropped metal ball, c) the modeled AE source in the form of the Hsu-Nielsen source.

For the recorded signals, there were calculated the mean values $U_{\mathrm{rms}}(x)$ and the average standard deviations $\sigma(x)$ of the mean values $U_{\mathrm{rms}}(x)$ for the signals in each measurement channel x (x is the number of the measurement channel). Next, there were calculated the mean values U_{rms} (for the mean values $U_{\mathrm{rms}}(x)$ expressed in dB). Finally, the values of $\Delta K_u(x)$ were determined and calculated: $\Delta K_u(x)$ is defined as the difference between the mean values $U_{\mathrm{rms}}(x)$ and U_{rms}.

An exemplary result of calibration for the measuring system with seven D9241A AE sensors and one R6 AE sensor is presented below. Such a choice of sensors enables illustrating significant issues occurring during the calibration process.

In Table 1, there are listed the mean values $U_{\mathrm{rms}}(x)$ and the average standard deviations $\sigma(x)$ of the mean values $U_{\mathrm{rms}}(x)$ calculated for ten signals recorded in individual measurement channels (x is the number of the measurement channel) during the calibration procedure. The quantities are expressed in mV. There are also given $\sigma(x)$ expressed in %, the mean value U_{rms} expressed in dB and the values of $\Delta K_u(x)$.

Table 1. Quantities describing the measuring system calibration by the Hsu-Nielsen method.

U_{rms} – average values, σ – standard deviations for U_{rms}, ΔK_u – corrections of gains										
Meas. channel	AE sensor type no.	AE sensor SN	Preampl. number	Amplific. [dB]	U_{rms} [mV]	σ [mV]	σ [%]	U_{rms} [dBmV]	ΔK_{u1} [dB]	ΔK_{u2} [dB]
CH0	D9241A	AJ88	0	20	**4.52**	0.47	10.50	73.11	**1.78**	**−0.19**
CH1	D9241A	AJ89	1	20	**4.87**	0.51	10.60	73.75	**1.14**	**−0.83**
CH2	D9241A	AJ93	2	20	**5.50**	0.43	7.74	74.81	**0.08**	**−1.89**
CH3	D9241A	AJ91	3	20	**9.54**	0.20	2.07	79.59	**−4.70**	∗
CH4	D9241A	AJ92	4	20	**4.19**	0.52	12.40	72.44	**2.45**	**0.48**
CH5	D9241A	AH91	5	20	**10.04**	0.24	2.35	80.04	**−5.15**	∗
CH6	D9241A	AI04	6	20	**3.35**	0.47	13.90	70.50	**4.39**	**2.42**
CH7	R6		7	20	**9.46**	0.36	3.76	79.51	∗	∗

∗ – **not applicable**

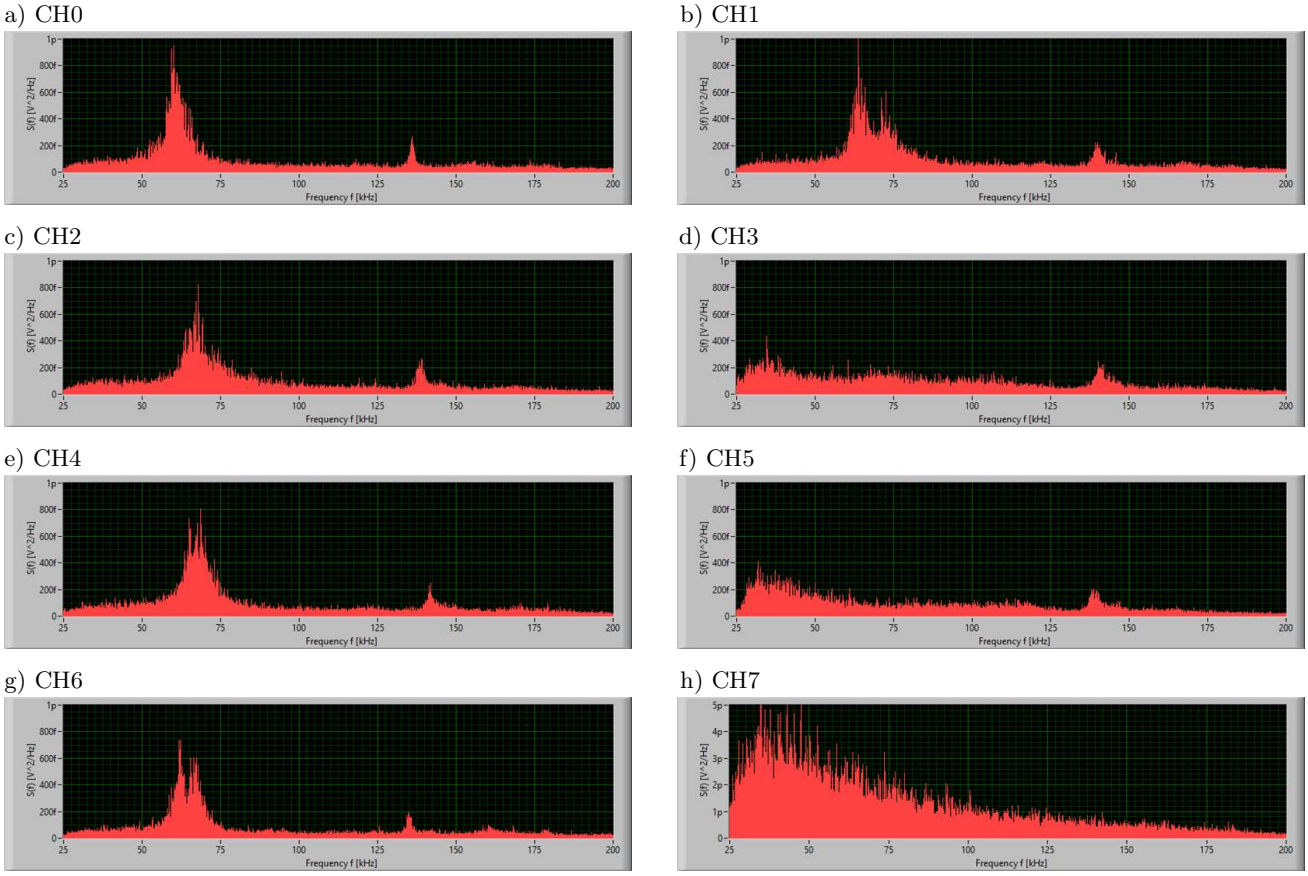

Fig. 5. Amplitude-frequency characteristics of the noises recorded in measurement channels CH0–CH6 with the D9241A sensors and in channel CH7 with the R6 sensor.

In the column ΔK_{u1}, there are presented the values of corrections in individual measurement channels in which the D9241A AE sensors were installed. Such a value was not calculated for the measurement channel CH7 with the R6 sensor, since the amplitude comparison of the signals recorded in measurement channels with different types of sensors is of limited value when describing phenomena. It is worth noting that the spread of the values of $\Delta K_{u1}(x)$ is greater than ± 3 dB, which in accordance with the standard (EN-13477, 2010) means that before performing investigations one should made the appropriate correction of the gains in individual channels.

Figure 5 presents the amplitude-frequency characteristics of the noises recorded in the measurement channels CH0-CH6 with the D9241A AE sensors. The detailed analysis of these characteristics shows that among the D9241As used in the measurements one can distinguish two subtypes with different characteristics. The sensors in the measurement channels CH0–CH2, CH4 and CH6 (with serial numbers: AJ88, AJ89, AJ93, AJ92, AI04, respectively) belong to the first subgroup. The other two AE sensors from the measurement channels CH4 and CH6 (with serial numbers: AJ91 and AH91) create the second subgroup.

In the column ΔK_{u2}, there are given the calculated values of the corrections in particular measurement channels with the AE sensors from the first subgroup. It should be noted that the spread of the values of $\Delta K_{u2}(x)$ is within the range ± 3 dB around the mean value, which in accordance with the standard (EN-13477, 2010) means that the correction is not necessary. Thus, the selection of AE sensors from one subgroup causes that the constructed measuring system complies to the requirements of the standard (EN-13477, 2010) without the need for correction of the gains in individual measurement channels. This conclusion is information about the compliance of measurement channels in the measuring system

4. Testing of the measuring system 8AE-PD

The testing of the measuring system by the Hsu-Nielsen method was carried out on a measuring stand equipped with a steel plate with modeled attenuation solutions. AE sensors were placed in distances of 50 cm and 100 cm from the Hsu-Nielsen source (Fig. 6).

Figure 7 shows the signals recorded in the two measurement channels for which the AE sensors were located at different distances from the Hsu-Nielsen source. In both signals, there are two structures with distinctly different amplitudes. In both cases, the amplitude in the first structure is a few times lower than that in the second structure. The duration of the first structure recorded by the sensor located 100 cm from the source is longer than the duration of this structure recorded by the sensor located 50 cm from the source.

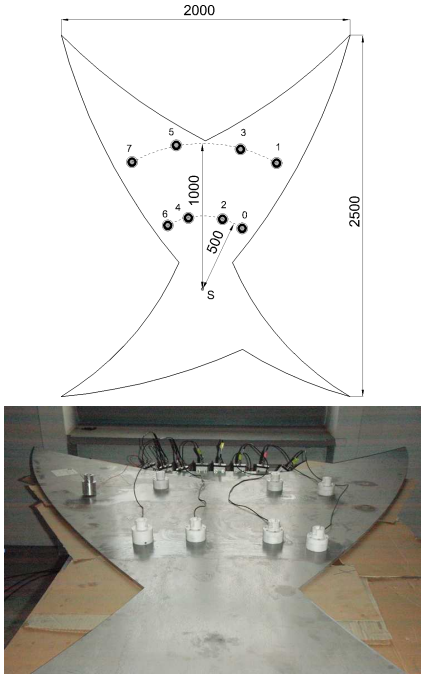

Fig. 6. Arrangement of AE sensors on the surface of the steel plate during testing of the measuring system: 0–7 positions of AE sensors, S – position of the Hsu-Nielsen source.

The detailed analysis of the arrival times of signals within the distinguished structures gives the following estimates: $t_{S0} = 0.090$ ms, $t_{A0} = 0.155$ ms. Because the difference in distance between the AE sensors is 0.5 m, then the determined differences of the arrival times within the distinguished structures give the following velocities for propagation of waves during the test:

- the pulse within the first structure propagates at a velocity of approx. 5.5 km/s,
- the pulse within the second structure propagates at a velocity of 3.2 km/s.

If one takes into account:

- the steel plate with the modeled attenuating shapes used for the performed investigations is thin (10 mm thick) and made of structural steel (velocity of transverse wave propagation – approx. 3230 m/s, velocity of longitudinal wave propagation – 5940 m/s),
- Lamb waves occur in such the plate,

then the calculated group velocity for the symmetric mode S0 equals 5432 m/s, while for the asymmetric mode A0 is 3007 m/s (at the fundamental frequency of 150 kHz).

The measured during the test and calculated values of the velocities for the considered modes are close to each other, so the case presented in Figs. 6 and 7 describes well the properties of the signals generated in plates by the Hsu-Nielsen method.

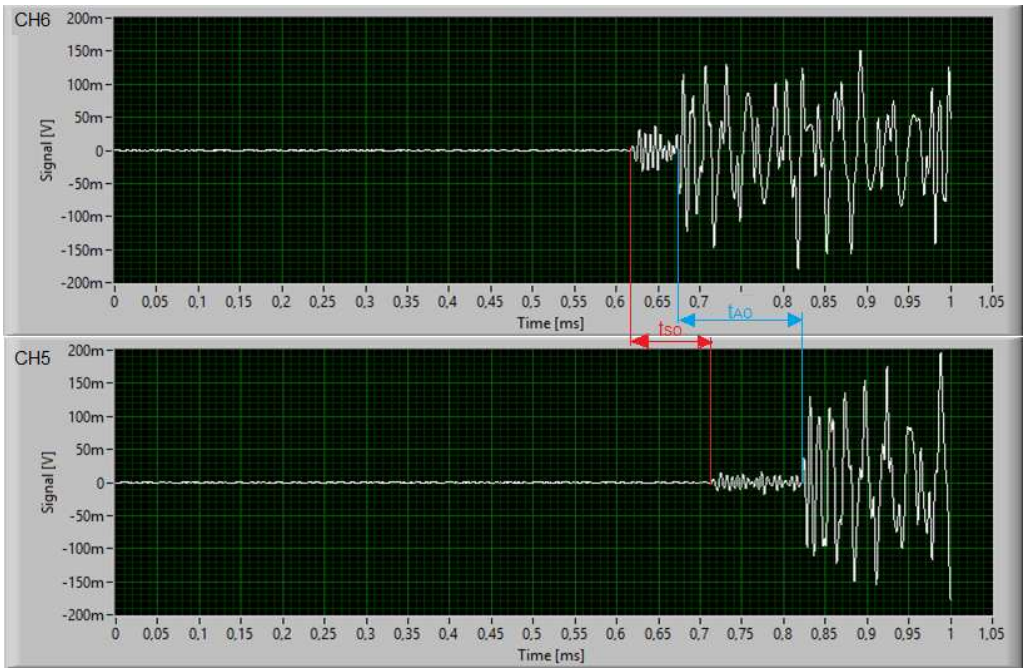

Fig. 7. Delay of the signals recorded in measurement channels CH6 and CH5.

5. Investigations of partial discharges in systems with a modeled source

5.1. Description of investigations

Investigations of PDs coming from a modeled source were performed in parallel by two methods: the AE method – with the use of the constructed measuring system 8AE-PD and the electrical method with the use of the PD measuring system of type TE 571 produced by Haefely Trench Tettex Instruments (Gacek *et al.*, 2011; Duda *et al.*, 2014). The investigation results obtained from the electrical method, particularly the measurement of the apparent charge introduced by the PD source are the reference for the results from the acoustic emission method. In (Witos, Gacek, 2008; 2009), such a methodology is named as the calibrated acoustic emission.

The investigations were carried out on the measurement stand whose schematic diagram is shown in Fig. 8. This stand includes: a test set generating high voltage (with a protection and regulation system), the computer PD measuring system using the electrical method equipped with a TE 571 measuring instru-

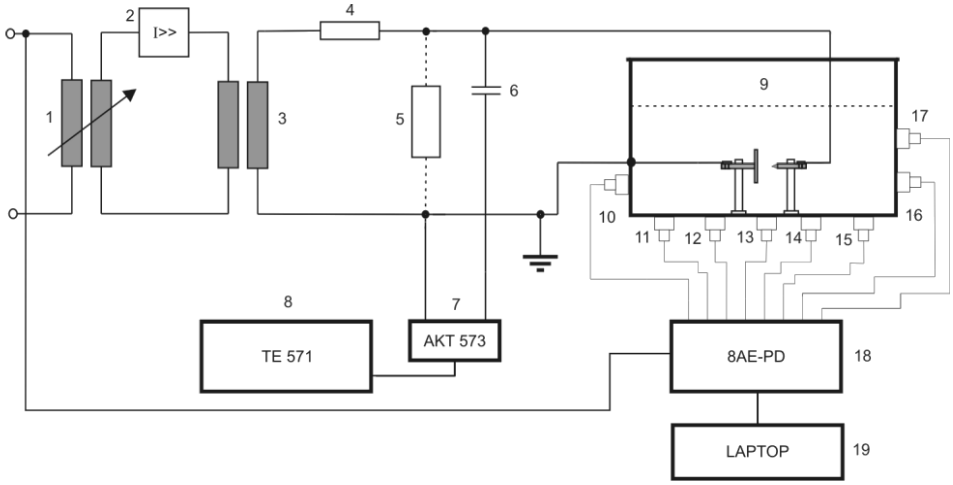

Fig. 8. Schematic diagram of the system for generating and testing PDs by the electrical and acoustic methods; 1 – autotransformer, 2 – overcurrent protection, 3 – high voltage transformer, 4 – protective resistance, 5 – calibrator KAL 451, 6 – coupling capacitor, 7 – coupling four-terminal network AKT 573, 8 – TE571 system, 9 – tank with the PD source, 10-17 – AE sensors, 18 – measuring system 8AE-PD, 19 – recording computer.

ment with additional equipment, a steel tank in the form of a cuboid with dimensions of $58 \times 110 \times 60$ cm (width × length × height), a modeled PD source and the measuring system 8AE-PD.

A constructed needle-plate spark gap was the modeled PD source. The spark gap was immersed in transformer oil. A view of the spark gap together with the elements inside the tank is shown in Fig. 9. The made spark gap consisted of a textolite base and supports on which metal electrodes, needle and plate, were mounted. PDs occurred in oil between the needle and the plate. The thus constructed spark gap can be regarded as a stable PD source (Skubis, 1993).

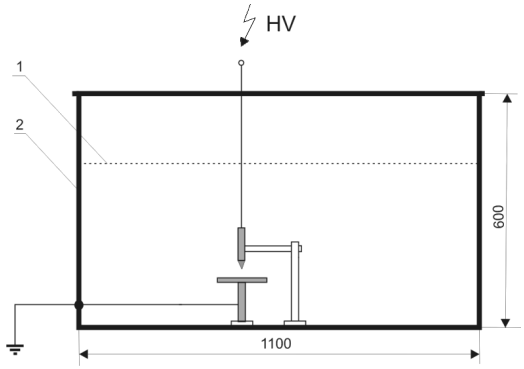

Fig. 9. Scheme of the tank with the modeled PD source together with the arrangement of elements inside the tank: 1 – level of transformer oil, 2 – steel tank.

The AE sensors were placed at selected points on the outside wall of the tank (Fig. 10) using magnetic holders. A coupling layer of technical vaseline provided the acoustic contact.

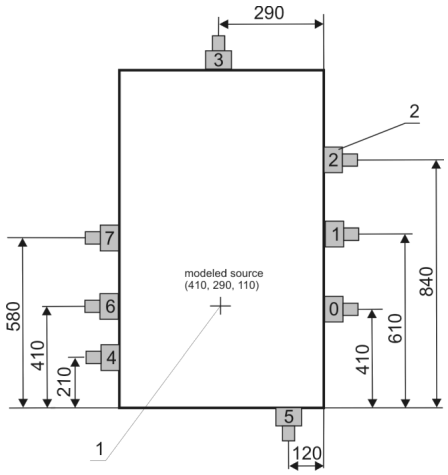

Fig. 10. Arrangement of AE sensors on the walls of the tank filled with transformer oil – top view showing the location of AE sensors No. 0–7 on the side walls (2) and the modeled PD source (1); coordinates of the sensors and source given in mm.

The measurement procedure consisted of 21 measurement series during which the value of the voltage applied to the spark gap was changed. The measurements were made by the AE and electrical methods.

During the investigations by the AE method – for successive values of the voltage applied to the spark gap – the signals were simultaneously recorded in all the measurement channels of the system 8AE-PD. In the reference measurement channel of the system 8AE-PD, phase-synchronized with HV supply voltage was also recorded.

The duration of the recorded signals was 1 second (about 20 periods of the supply voltage). The recording was carried out several times and the data were written to datasets. The measuring system 8AE-PD contained six measurement channels with D9241A AE sensors and two measurement channels with wide band AE sensors.

During investigations by means of the electrical method for obtaining PD with different value of apparent charge involved by modeled source, the value of the voltage applied to the spark gap were changed. Since the supply voltage is periodic in Table 2, U values mean effective values of this periodic supply voltage. For each U, the mean value of the apparent charge introduced by the modeled source per cycle as well as the average current of PD and the average number of PDs per second were measured. These results are shown in Table 2 as Q, I and N.

Table 2. Summary of test results obtained by means of electrical method.

No.	U [kV]	Q [pC]	I [nA]	N [1/s]
1	21.9	3	1	1000
2	22.4	6	0.5–0.7	500
3	22.9	8	0.3	50–60
4	23.4	20	0.6	47–70
5	24.4	70	3	70
6	24.9	120	8–10	90–103
7	24.9	120	8–10	90–103
8	24.9	120	8–10	90–103
9	24.9	120	5–7	55
10	24.9	120	5–7	55
11	25.4	130	6.5	60–105
12	25.4	130	5–7	50–80
13	25.4	130	5–7	50–80
14	25.9	180	9–12	90–125
15	25.9	180	9–12	90–125
16	25.9	180	9–12	90–125
17	27.5	260	11–20	119–130
18	29.5	380	35–40	220–260
19	0	0	0	0
20	0	0	0	0
21	0	0	0	0

From Table 2 one can see that the values of the apparent charge introduced by the modeled PD source were contained in the range from 0 to 380 pC.

5.2. General properties of the AE signals coming from PDs

The basic description of the exemplary AE signal recorded in the measurement channel with the wide band AE sensor for the case of introducing the apparent charge of the value 380 pC by the modeled source is shown in Fig. 11. Such a description contains analysis in time, frequency and time-frequency domains (Witos, 2008; Witos, Gacek, 2013). The recorded signal has periodic and stochastic properties due to the complexity of the processes occurring during initiation and maintenance of PDs. The periodicity of the PD phenomena is confirmed by the facts the signals occur twice during the period of the supply voltage, which is shown by:

- two "tunnels" on the phase-time characteristic (Fig. 11e),
- two maxima on the averaged phase characteristic (Fig. 11d),
- two spatial peaks occurring within three different frequency bands within the averaged spectrogram (Fig. 11f).

The stochastic nature is reflected within the fluctuations of the amplitudes in Figs. 11a and 11e for different periods of supply voltage.

According to the frequency characteristic (Fig. 11b), the signal has the following dominant bands: 32–35 kHz, 49–53 kHz and 82–92 kHz. The averaged Short Time Fourier Transform (STFT) spectrogram (Fig. 11f) confirms these dominant bands but it also shows the band 155–175 kHz.

In Table 3, the properties of the AE signals coming from PDs (for the apparent charges of the mean values 380 and 120 pC introduced by the modeled

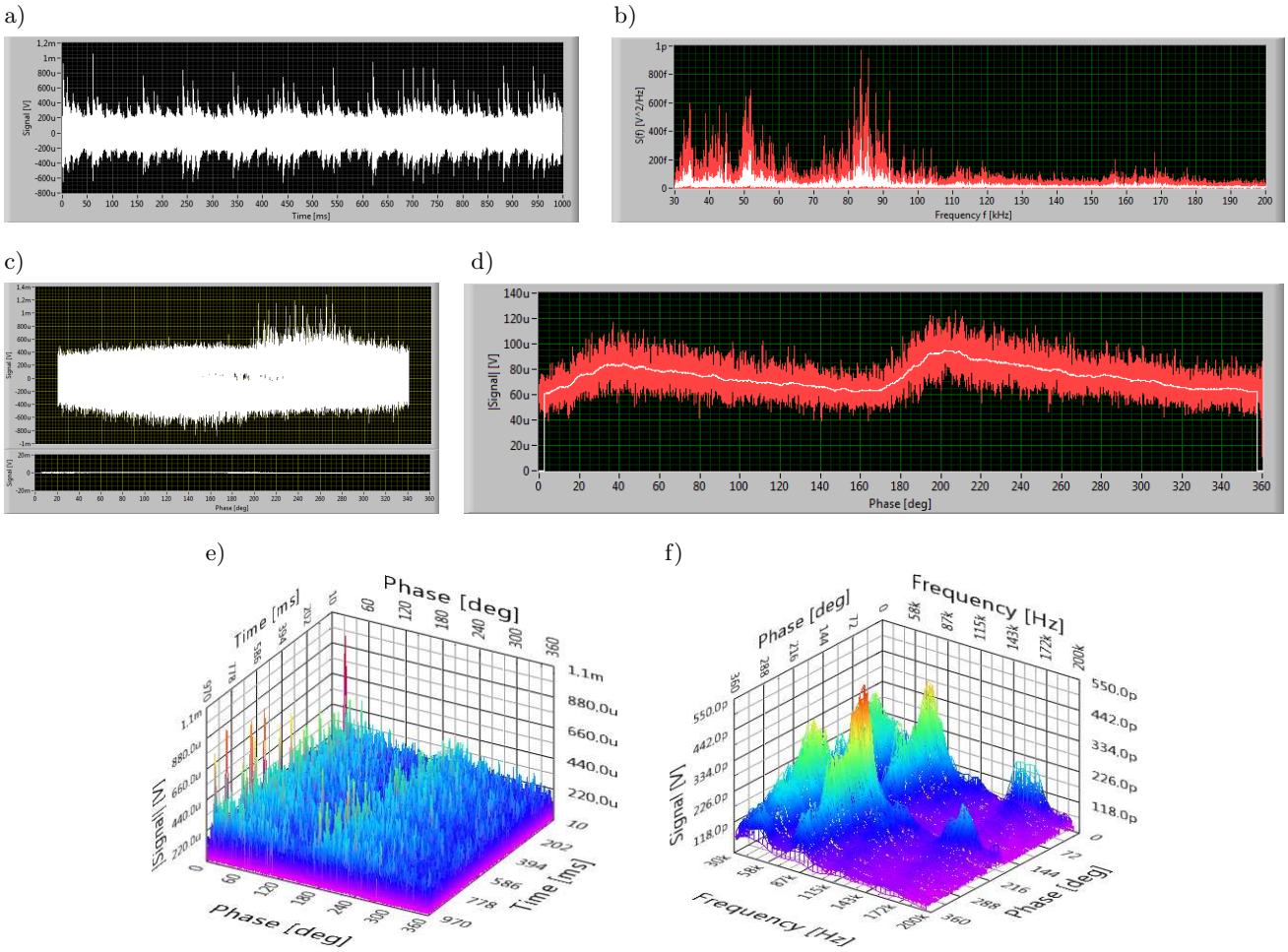

Fig. 11. Basic description of the AE signal recorded in measurement channel CH6 (with the wide band AE sensor) at measurement conditions $U = 29.5$ kV, $Q = 380$ pC: a) signal after filtration ($U_{\max} = 1.16$ mV, $U_{\min} = -1.07$ mV, $U_{\rm rms} = 159.3$ µV), b) characteristic of signal spectral power [V^2/Hz] vs. frequency [Hz] ($f_{\max} = 83.5$ kHz, $U^2_{\rm rms}(f_{\max}) = 2.24$ pV^2), c) signal phase characteristic, d) averaged phase characteristic, e) phase-time characteristic, f) averaged STFT spectrograms.

Table 3. Properties of the AE signals from PDs and noises.

Parameter	Designation	Unit	The measurement series		
			$Q = 0$ pC $U = 0.0$ kV Noise_46 dB	$Q = 120$ pC $U = 24.9$ kV P5_46 dB	$Q = 380$ pC $U = 29.5$ kV P22_46 dB
			The results of the calculated parameters		
Maximum value of amplitude of AE signal $U(t)$	$U_{\max}$	mV	88.5	132.3	236.4
Minimum value of amplitude of AE signal $U(t)$	$U_{\min}$	mV	−86.2	−146.7	−210.4
Average value of the AE signal $U(t)$	U_{av}	μV	95.2	−123.1	−180.1
RMS value of the signal $U(t)$	U_{rms}	mV	18.7	27.4	31.9
Average value of the module of AE signal $U(t)$	$\|U\|_{\text{av}}$	mV	8.6	17.8	26.7
Average standard deviation of the average value of AE signal $U(t)$	S_u	mV	14.9	18.9	28.1
Distribution coefficient of AE signal	$K = S_u/\|U\|_{av}$	–	1.73	1.06	1.05

source) and noises are presented. These signals were recorded within measurement channel with wide band AE sensor. There are a few magnitudes describing registered AE signals: maximum value $U_{\max}$, minimum value $U_{\min}$, average value U_{av}, average value of the module $|U|_{\text{av}}$, average standard deviation of the average value S_u and distribution coefficient K of AE signals $U(t)$.

Such a distribution coefficient K of AE signals $U(t)$ which is a quotient of S_u and $|U|_{\text{av}}$ gives distinguishing between signals and noises. In case of analyzed AE signals $U(t)$ the calculated distribution coefficients K are following:

- for the AE signals recorded at the active PD source: $K = 1.06$ (for $Q = 380$ pC,) and $K = 1.05$ (for $Q = 120$ pC), respectively,
- for the noise $K = 1.73$.

Values of K equal 1.05 and 1.06 are typical for information, whereas value K equals 1.73 describes the noises. Therefore, these results confirm quantitatively the possibility of a measuring system for distinction between noise and signal generated by the modeled source of PD.

Before detailed analyzing of the recorded signals, there were additionally analyzed from the point of view of the velocity of the AE waves propagating in the investigated object. Figure 12 shows the AE pulses from PDs generated by the modeled source. The pulses were recorded by the AE sensors in measurement channels CH0–CH3. In Fig. 12, one can see increasing values of the time of the AE signal arrival at successive sensors. It's in accordance with the fact, the AE signals generated in the source reached successive AE sensors after propagating within paths of increasing length in transformer oil (location of the sensors and the source is shown in Fig. 10).

Estimation of the difference of the arrival times at sensors CH3 and CH0, and hence determination of the velocity of the longitudinal wave in the transformer oil used in the investigations gives the value of approx. 1380 m/s. This value is close to the literature value of 1390 m/s for the velocity of the longitudinal wave in oil at the temperature of 20°C (Skubis, 1993).

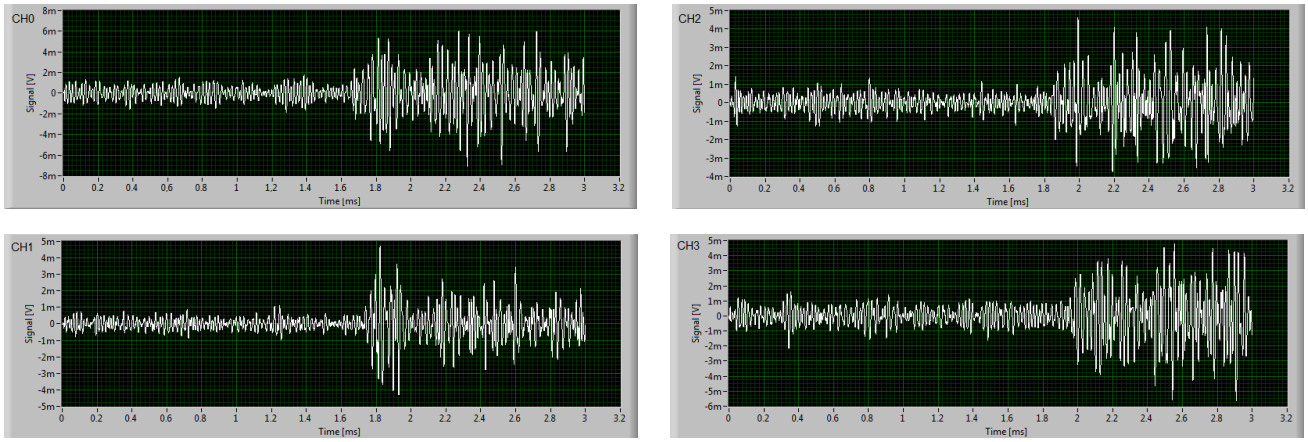

Fig. 12. AE signals recorded in measurement channels CH0-CH3.

5.3. Determination of measurement possibilities of the measuring system 8 AE-PD

For the signals recorded during the investigations of PDs from the modeled source, for each measurement serie, there were calculated the mean values of the peak-to-peak voltage U_{mm} and the RMS voltage of the signal U_{rms} and the average standard deviations of the so calculated magnitudes. Results of those calculations are presented in Figs. 13 and 14 where there are shown the characteristics $U_{\mathrm{mm}}(Q)$ and $U_{\mathrm{rms}}(Q)$ for the measurement channels CH0 and CH6, where the independent variable is expressed on a logarithmic scale. These characteristics show the relationship between the signal quantities U_{mm} and U_{rms} measured by the AE method and the value of the apparent charge Q introduced by the PD source measured by the electrical method. Since the values of the apparent charge introduced by the source are contained in three ranges, namely 1–10–100–1000 pC, the scale for the independent variable on the charts $U_{\mathrm{mm}}(Q)$ and $U_{\mathrm{rms}}(Q)$ is logarithmic. With this approach, the waveforms of the curves of Figs. 13 and 14 are similar: one can distinguish a flat part (part No. I), next the values of the quantities U_{mm} and U_{rms} slightly increase (part No. II), and after that they radically increase (part No. III). One can determine the intersection point of the parts I and III on the particular curves. The coordinates of the so determined points on the Q axis are as follows:

- value Q_g (U_{mm}, sensor D9241A) = 150 pC,
- value Q_g (U_{rms}, sensor D9241A) = 200 pC,
- value Q_g (U_{mm}, sensor WD) = 200 pC,
- value Q_g (U_{rms}, sensor WD) = 250 pC.

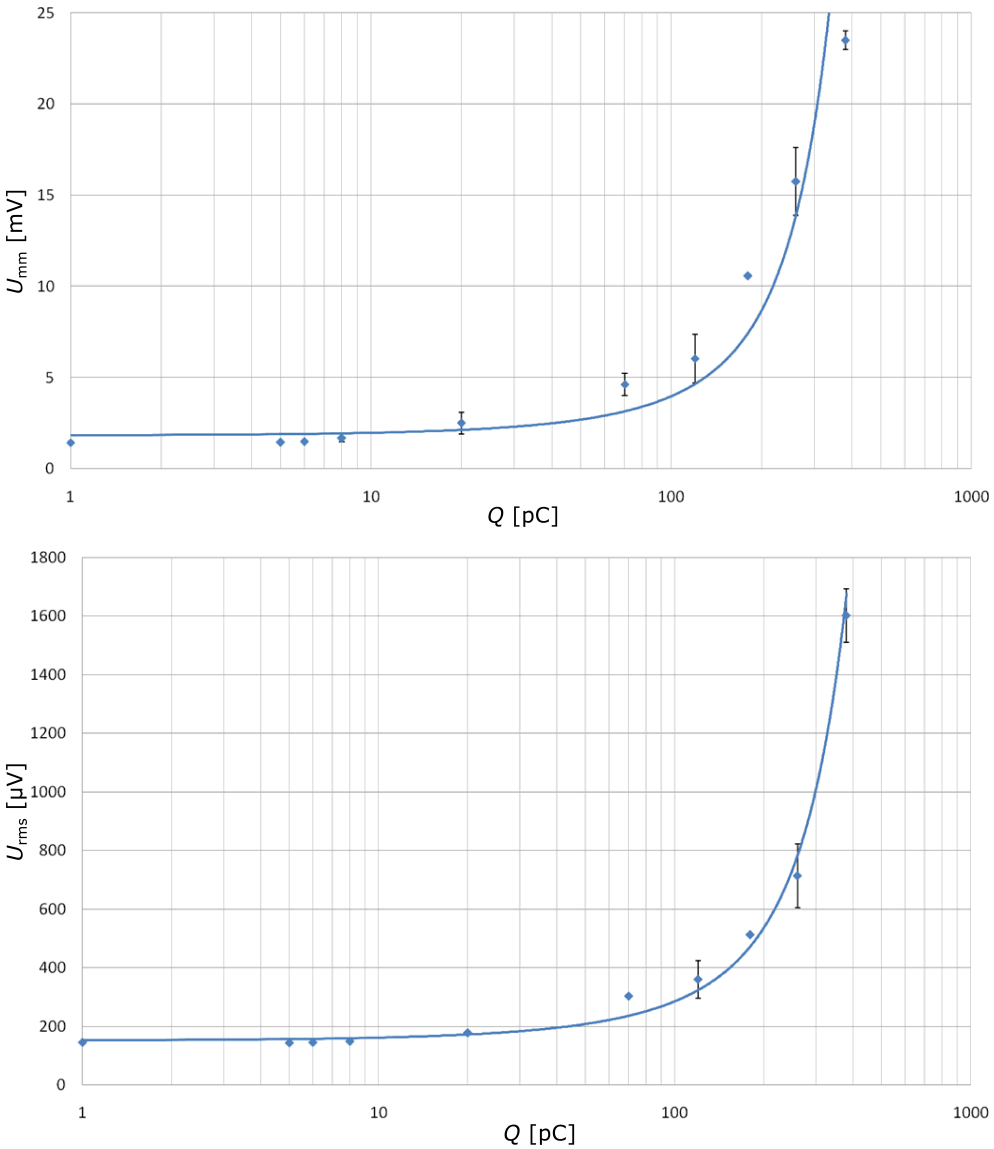

Fig. 13. Characteristics $U_{\mathrm{mm}}(Q)$ and $U_{\mathrm{rms}}(Q)$ describing the AE signals recorded during 21 measurement in measurement channel CH0 (with the D9241A resonant AE sensor).

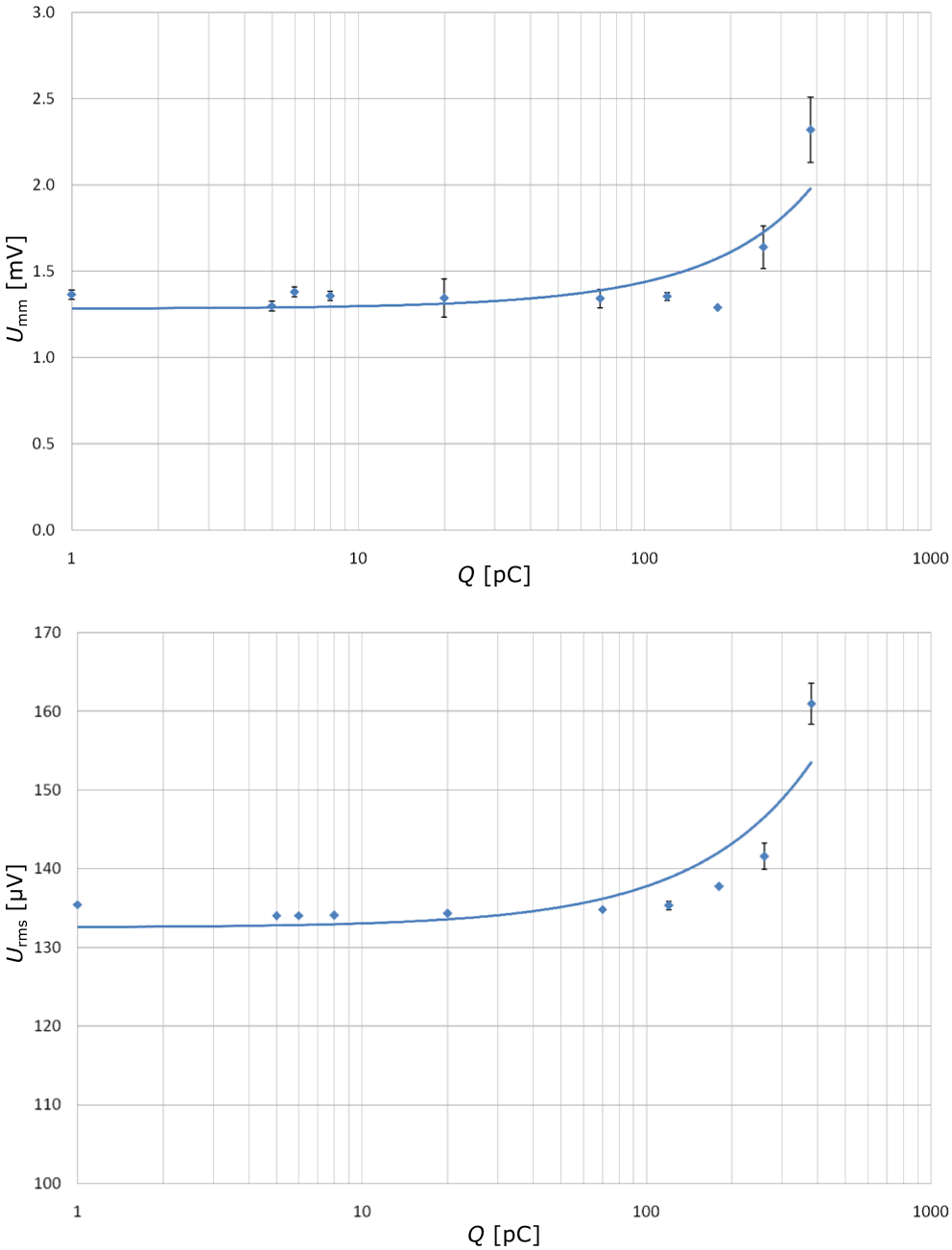

Fig. 14. Characteristics $U_{\mathrm{mm}}(Q)$ and $U_{\mathrm{rms}}(Q)$ describing the AE signals recorded during 21 measurement series in measurement channel CH6 (with the WD wide band AE sensor).

However, so determined values do not specify the limit minimum value of the apparent charge introduced by the source for which the recorded signal will be identified as that originating from PDs. This conclusion is confirmed in Fig. 15, where there are depicted the AE signals recorded in measurement channel CH0 (with the D9241A AE resonant sensor) during introducing charges of different values by the modeled PD source. From Fig. 15, it follows that the PD phenomenon recorded by the AE method can be observed for the active PD source introducing the apparent charge of 70 pC, and this phenomenon recorded by the AE method is still visible for the apparent charge value of 20 pC.

In order to precisely determine the limit minimum value of the apparent charge introduced by the source for which the recorded signal will be identified as that originating from PDs, analysis of the recorded signals by using method of AE descriptors of acronyms ADP and ADC defined and presented by authors (Olszewska, Witos, 2012; Witos, Gacek, 2013) has been carried out.

To calculate these descriptors for the recorded signals the following procedure is appropriate: signals are

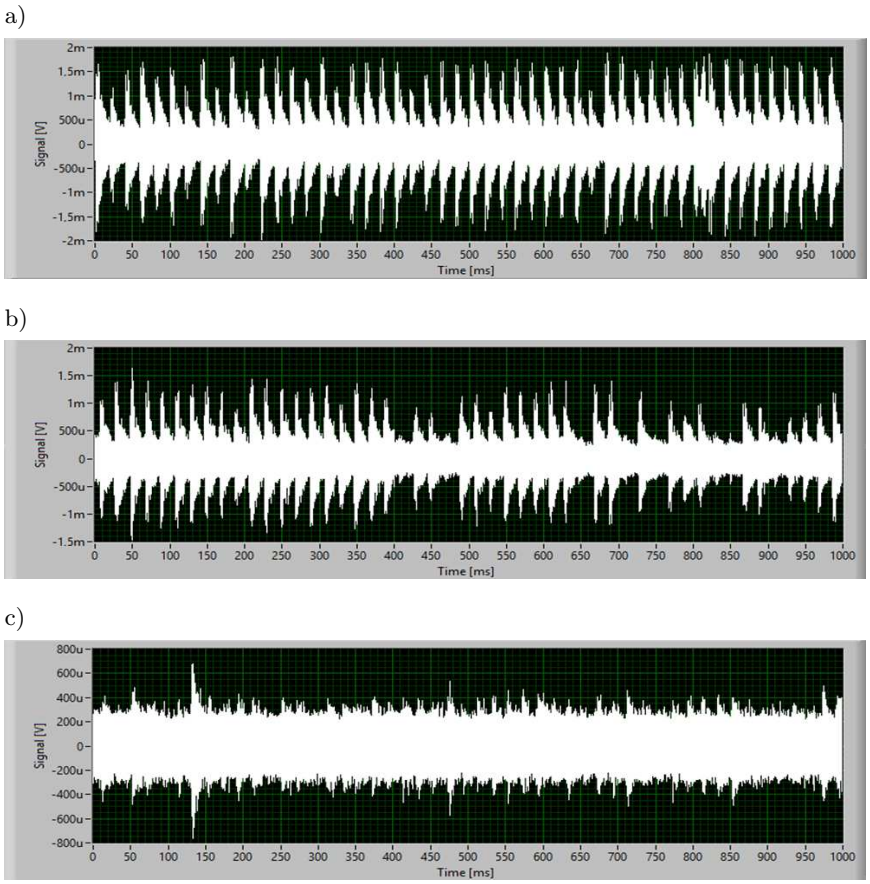

Fig. 15. AE signals recorded in measurement channel CH0 (with the D9241A resonant AE sensor) during introducing charges of different values by the modeled PD source: a) $Q = 120$ pC, b) $Q = 70$ pC, c) $Q = 20$ pC.

filtered within defined frequency band (Witos, Opilski, 2012), then there are created amplitude distributions for the signal power (**A**mplitude **D**istribution of AE signal **P**ower) and count rate (**A**mplitude **D**istribution of AE **C**ounts). Then, the appropriate parts of the amplitude distributions constructed in a logarithmic scale are approximated by a straight line and the slopes of such straight lines are the descriptor values; eg. for count rate

$$\ln\left(\frac{\mathrm{d}N(U)}{\mathrm{d}t}\right) = AU + B, \qquad A = ADC.$$

The defined descriptors have the following properties:

- not based on absolute values measured signals EA,
- take negative values and greater value of descriptor corresponds more closely "the flat" character of the distribution of amplitude,
- admit for registered signals the so-called degree of advancement according to the rule "greater value descriptor is a higher degree of signal degree advancement,
- allow for distinction of phenomena related to the propagation of elastic wave in a material and in coupling layer (by application of a logarithmic scale in the graphs of amplitude distributions).

For the signals recorded during the investigations of the PDs from the modeled source, the mean values of the descriptors ADP and ADC as well as the average standard deviations of these descriptors were calculated for the individual measurement series.

Results of those calculations are presented in Fig. 16 where there are shown the characteristics ADP(Q) and ADC(Q) for the measurement channels CH0 and CH6, where the independent variable is expressed on a logarithmic scale. These characteristics show the relationship between the descriptors ADC and ADP calculated for the signals from PDs measured by the AE method and the value of the apparent charge Q introduced by the PD source measured by the electrical method.

It is worthwhile to compare the curves of Fig. 16a with the curves from Figs. 13a and 14a, and the curves in Fig. 16b with curves from Figs. 13b and 14b. It is a comparison of two descriptions of the properties of the signals recorded: through ADC, ADP descriptors and through U_{mm}, U_{rms} descriptors.

Detailed analysis of the shape of the curves from Figs. 13, 14 and 16 leads to the conclusion that descrip-

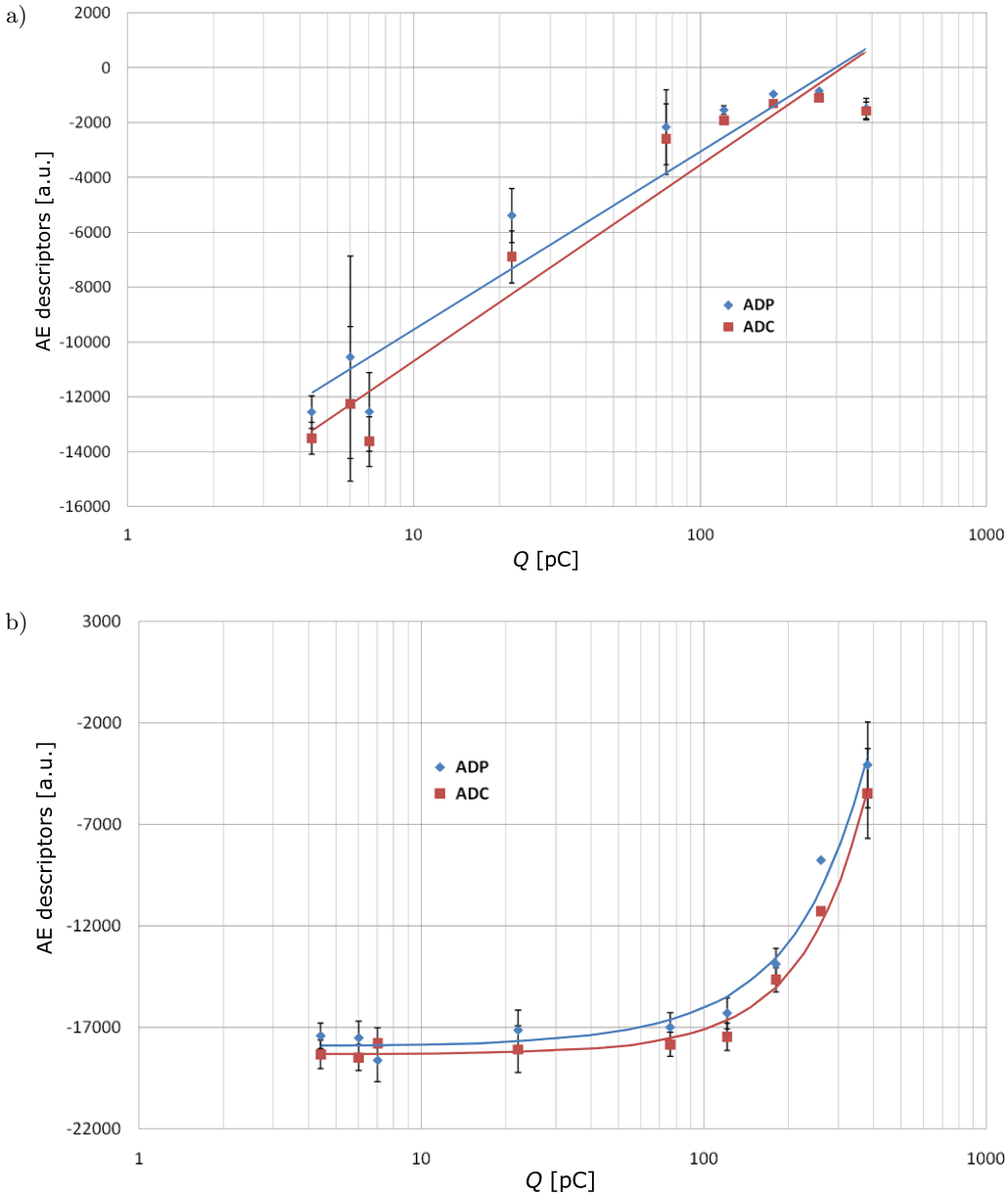

Fig. 16. Characteristics ADP(Q) and ADC(Q) describing the AE signals recorded during 21 measurement series: a) in measurement channel CH0 (with the D9241A AE resonant sensor), b) in measurement channel CH6 (with the WD wide band AE sensor).

tion through ADC, ADP descriptors is more sensitive than description through U_{mm}, U_{rms} descriptors. For signals recorded in the measurement channel containing wideband AE sensors curves have similar shapes. For signals recorded in the measurement channel containing resonance AE sensor (with the band being the dominant band of PDs) shape of the curves is different. This difference means that, in this case, the amplitude distributions for AE signals from the PD source introducing apparent charge of 20 pC differ fundamentally from the amplitude distribution of the noise signals.

Determination of the limit minimum value of the apparent charge introduced by the source for which the recorded signal will be identified as that originating from PDs on the curves ADP(Q) and ADC(Q) is much more obvious and one can assume that:

- values Q_g (ADP, sensor D9241A) and Q_g (ADC, sensor D9241A) are equal approx. 20 pC,
- values Q_g (ADP, sensor WD) and Q_g (U_{rms}, sensor WD) are equal approx. 150 pC.

6. Conclusion

In the paper, the general description of the constructed measuring system 8AE-PD has been presented.

There was developed the methodology, followed by the calibration of the measuring system using the Hsu-Nielsen method. As a result of the calibration, there was made the amplitude correction in the form of the calculated values of the gain corrections $\Delta K_{u1}(x)$ for the particular measurement channels x. The made calibration enables using the system for investigations of AE signals by the largest volume method as well as using triangulation methods when locating the sources of AE signals.

The system was tested when generating a signal by Hsu-Nielsen sources in a steel plate, identifying the recorded signals as the basic antisymmetric $A0$ and symmetric $S0$ modes, as well as when generating a signal by the modeled PD source, identifying the recorded signals as the longitudinal volume waves propagating in transformer oil.

A modeled PD source in the form of a needle-plate spark gap was constructed. The PDs generated by such a source were investigated on a measurement stand built for this purpose. The acoustic emission method and the electrical method were used in parallel for investigations. The values of the apparent charge introduced by the modeled PD source were contained in the range from 0 to 380 pC. The results obtained from the acoustic emission method were referred to those obtained from the electrical method.

For the AE signals generated by PD source introducing apparent charge with value of 380 pC following characteristics: amplitude vs. frequency, amplitude vs. phase, averaged amplitude vs. phase, amplitude vs. phase in subsequent periods of the supply voltage and averaged STFT spectrograms are presented. The possibility of a measuring system for distinction between noise and signal generated by the modeled source of PD are shown quantitatively.

The descriptions of the properties of the AE signals generated by PDs through U_{mm}, U_{rms} descriptors and through descriptors ADC, ADP and analysis of curves $U_{\mathrm{mm}}(Q)$, $U_{\mathrm{rms}}(Q)$, ADC(Q) and ADP(Q) have been presented in the paper. Detailed analysis determined the limit values of the apparent charge introduced by the PD source for which the recorded signal is identified as that coming from PDs and allowed to draw the conclusion that description through ADC, ADP descriptors is more sensitive than description through U_{mm}, U_{rms} descriptors and gave information that for signals recorded in the measurement channel containing resonance AE sensor (with the band being the dominant band of PDs) it is possible to identify signal generated by modeled PD source introducing apparent charge with value of 20 pC.

References

1. Boczar T. (2001), *Identification of specific type of PD from AE frequency spectra* IEEE Trans. on Dielectric and Electrical Insulation, **8**, 4, 598–606.
2. Duda D., Maźniewski K., Szadkowski M. (2014), *The complementary use of methods of electric and acoustic to analyze the modeled sources of partial discharges* [in Polish], Przegląd Elektrotechniczny, **90**, 10, 129–132.
3. EN 13477-2:2010 *Non-destructive testing – Acoustic emission – Equipment characterisation – Part 2: Verification of operating characteristic.*
4. Gacek Z., Szadkowski M., Malitowski G., Witos F., Olszewska A. (2011), *Anusual application of partial discharges to diagnose of high voltage power transformers*, Acta Phys. Pol. A, **120**, 4, 609–615.
5. Hsu N., Breckenridge F. (1981), *Characterization and calibration of AE sensors*, Materials Evaluation, **39**, 1, 60–69.
6. MacAlpine M., Zhiquiang Z., Demokan M.S. (2002), *Development of a fibre-optic sensor for PDs in oil-filled power transformers*, Electric Power System Research, **63**, 1, 27–36.
7. Malecki I., Witos F., Opilski A. (1993), *AE source parameters in coal samples*, Acustica, **79**, 2, 112–116.
8. Meissner M., Ranachowski Z. (1992), *Generation and propagation of standard pulses of acoustic emission* [in Polish: *Generacja i propagacja wzorcowych impulsów emisji akustycznej*], Prace IPPT, **36**, Warszawa.
9. Olszewska A., Witos F. (2011), *Location and identification of acoustic signals recorded in power oil transformers within the band of 20–180 kHz*, Acta Phys. Pol. A., **120**, 4, 709–712.
10. Olszewska A., Witos F. (2012), *Location of partial discharge sources and analysis of signals in chosen power oil transformers by means of acoustic emission method*, Acta Phys. Pol. A., **122**, 5, 921–926.
11. Opilski A., Witos F., Ranachowski J., Ranachowski Z. (1985), *Applications of AE for the investigations of stresses in geological materials*, Acoustics Letters, **8**, 7, 109–114.
12. Sarathi R., Singh P.D., Danikas M.G. (2007), *Characterization of partial discharges in transformer oil insulation under DC and AC voltage using acoustic emission technique*, Journal of Electrical Engineering, **58**, 2, 91–97.
13. Skubis J. (1993), *Acoustic emission studies of insulation of electrical power devices* [in Polish], IPPT PAN, Warszawa.
14. Witos F., Opilski A., Lutyński A. (1989), *Investigations of AE pulses in horizontal transport belts used in mining, subject to uniaxial stresses*, Ultrasonics, **7**, 5, 182–185.
15. Witos F. (2008), *Investigation of partial discharges by means of acoustic emission method and electric method* [in Polish], Wydawnictwo Politechniki Śląskiej, Gliwice.
16. Witos F., Gacek Z. (2008), *Application of the joint electro-acoustic method for partial discharge investiga-*

tions within a power transformer, European Physical Journal: Special Topics, **154**, 1, 239–247.

17. Witos F., Olszewska A., Szerszen G. (2011), *Analysis of properties characteristic for acoustic emission signals recorded on-line in power oil transformers*, Acta Phys. Pol. A, **120**, 4, 759–762.
18. Witos F., Opilski Z. (2012), *The method of partial discharges locating, particularly in the power oil transformers, based on the map of acoustic emission descriptors in the frequency domain*, Patent: PL 223 605.
19. Witos F., Szerszen G., Setkiewicz M., Opilski Z., Gacek Z., Urbanczyk M. (2012), *The computer measuring system of acoustic emission signals 8AE-PD dedicated for partial discharges investigation* [in Polish], Przegląd Elektrotechniczny, **88**, 11b, 146–150.
20. Witos F., Gacek Z. (2013), *Testing of partial discharges and location of their sources in generator coil bars by means of acoustic emission and electric methods*, [in:] Acoustic Emission – Research and Applications, Sikorski W. [Ed.], Rijeka, InTech, 117–145.